*remote sensing*

MDPI

*Article*

# Modeling Carbon Emissions of Post-Selective Logging in the Production Forests of Ulu Jelai, Pahang, Malaysia

**Siti Nor Maizah Saad [1,2], Wan Shafrina Wan Mohd Jaafar [1,*], Hamdan Omar [3], Khairul Nizam Abdul Maulud [1,4], Aisyah Marliza Muhmad Kamarulzaman [1], Esmaeel Adrah [1], Norzalyta Mohd Ghazali [5] and Midhun Mohan [6]**

1 Earth Observation Centre, Institute of Climate Change, Universiti Kebangsaan Malaysia, Bangi 43600, Selangor, Malaysia
2 Arau Campus, Universiti Teknologi MARA Perlis Branch, Arau 02600, Perlis, Malaysia
3 Forest Research Institute Malaysia, Kepong 52109, Selangor, Malaysia
4 Department of Civil Engineering, Faculty of Engineering and Built Environment, Universiti Kebangsaan Malaysia, Bangi 43600, Selangor, Malaysia
5 Department of Biological Sciences and Biotechnology, Faculty of Science and Technology (FST), Universiti Kebangsaan Malaysia, Bangi 43600, Selangor, Malaysia
6 Department of Geography, University of California-Berkeley, Berkeley, CA 94709, USA
* Correspondence: wanshafrina@ukm.edu.my; Tel.: +60-3-89216941

**Abstract:** Harvested timber and constructed infrastructure over the logging area leave massive damage that contributes to the emission of anthropogenic gases into the atmosphere. Carbon emissions from tropical deforestation and forest degradation are the second largest source of anthropogenic emissions of greenhouse gases. Even though the emissions vary from region to region, a significant amount of carbon emissions comes mostly from timber harvesting, which is tightly linked to the selective logging intensity. This study intended to utilize a remote sensing approach to quantify carbon emissions from selective logging activities in Ulu Jelai Forest Reserve, Pahang, Malaysia. To quantify the emissions, the relevant variables from the logging's impact were identified as a predictor in the model development and were listed as stump height, stump diameter, cross-sectional area, timber volume, logging gaps, road, skid trails, and incidental damage resulting from the logging process. The predictive performance of linear regression and machine learning models, namely support vector machine (SVM), random forest, and K-nearest neighbor, were examined to assess the carbon emission from this degraded forest. To test the different methods, a combination of ground inventory plots, unmanned aerial vehicles (UAV), and satellite imagery were analyzed, and the performance in terms of root mean square error (RMSE), bias, and coefficient of correlation ($R^2$) were calculated. Among the four models tested, the machine learning model SVM provided the best accuracy with an RMSE of 21.10% and a bias of 0.23% with an adjusted $R^2$ of 0.80. Meanwhile, the linear model performed second with an RMSE of 22.14%, a bias of 0.72%, and an adjusted $R^2$ of 0.75. This study demonstrates the efficacy of remotely sensed data to facilitate the conventional methods of quantifying carbon emissions from selective logging and promoting advanced assessments that are more effective, especially in massive logging areas and various forest conditions. Findings from this research will be useful in assisting the relevant authorities in optimizing logging practices to sustain forest carbon sequestration for climate change mitigation.

**Keywords:** selective logging impacts; UAV; remote sensing; machine learning model; carbon emission



**Citation:** Saad, S.N.M.; Wan Mohd Jaafar, W.S.; Omar, H.; Abdul Maulud, K.N.; Muhmad Kamarulzaman, A.M.; Adrah, E.; Mohd Ghazali, N.; Mohan, M. Modeling Carbon Emissions of Post-Selective Logging in the Production Forests of Ulu Jelai, Pahang, Malaysia. *Remote Sens.* **2023**, *15*, 1016. https://doi.org/10.3390/rs15041016

Academic Editors: Arturo Sanchez-Azofeifa, Ehsan Khoramshahi and Francisco Javier Mesas Carrascosa

Received: 28 December 2022
Revised: 9 February 2023
Accepted: 10 February 2023
Published: 12 February 2023



## 1. Introduction

Selective logging operations degrade the forest volume and cause disturbance to the intact forest in most tropical regions. Massive and unmanaged logging activities result in the loss of forest above-ground biomass (AGB) due to damage to the trees and their surroundings. This increases the number of carbon emissions ($CO_2$) and greenhouse gas

(GHG) emissions into the atmosphere affecting the future global climate [1]. Although selective logging may cause less impact on carbon emissions from forest damage compared to other deforestation activities [2], it can still have a significant impact due to the frequency of logging [3,4]. Monitoring forest degradation from harvesting operations is essential in tropical forests to address the issues of forest carbon emissions and climate change [5]. Tropical forests constitute the largest portion of the world's forests, and the forest ecosystem stores more than 80% of terrestrial above-ground carbon, and timber harvesting operations contribute to 53% of the total carbon ($CO_2$) emissions that are released into the atmosphere [2].

The global framework of reducing emissions from deforestation and forest degradation (REDD+) was established to conserve and enhance carbon stock in developing countries. Malaysia's implementation of REDD+ is aimed at ensuring that the forest resources and their ecosystems are protected and that the benefits are shared equally among all the beneficiaries [6]. Malaysia is a timber-producing country that harvests timber trees selectively for their commercial value, utilizing sustainable management system (SFM) and selective management system (SMS) practices [7,8]. The data from [9] show that Malaysia has around 67.09% forested area, out of which 22.71% are diverse primary forests with dense carbon storage.

Selective logging is the process of harvesting a timber tree in a forest area that may change the forest landscape and structure. When the individual tree area is harvested, the forest suffers further damage resulting in various carbon pools [10]. Monitoring and assessing the carbon emissions caused by selective logging is part of the forest logging sustainability effort that aims to manage the operation, thus helping in the carbon emission reduction strategy. However, selective logging has both good and negative consequences on the release of carbon. The decrease in forest cover may result in a short-term increase in carbon emissions and a decrease in the capacity of carbon sinks. However, judicious logging may also boost the forest's carbon supply in the long term to encourage natural regeneration. Quantifying AGB and carbon stock from ground inventories at some stages can be challenging due to multiple factors such as operational cost, terrain conditions (especially in dense forest areas), seasonal variations, manpower, and site accessibility [11]. Nevertheless, the integration of ground investigation and remote sensing techniques has been utilized widely to provide accurate forest parameters for quantifying carbon stock and emissions [3]. To ensure that the assessment is robust, reliable, and practical, the ground sampling technique is combined with the remote sensing approach to overcome the limitations of using ground-based assessments alone [7,12].

Over the years, high-resolution and high-accuracy data have often been used in forest carbon-related studies due to their advance in sensors and capturing technologies. Digital aerial photos from unmanned aerial vehicles (UAV), light detection and ranging (LiDAR), and airborne multispectral and hyperspectral images are highly utilized in many sectors of forestry fields [13]. However, LiDAR data, although accurate and effective, is often challenging to obtain due to its high cost. Alternatively, UAVs have been found to provide a more cost-effective option and promising results at an affordable cost [14,15] and are widely utilized in forest research [12,16]. Research on post-harvesting logging impact on a variety of forest landscapes using a machine learning and automation approach to UAV data was conducted in several areas around the world [17–19]. In Malaysia, researchers utilized remote sensing—UAV based to estimate forest parameters and logging indicators for selective logging impacts, such as identifying left stump, logging gaps, and transportation infrastructures such as roads and skid trails [16,20,21].

Whereas many studies have investigated the carbon emission impact of selective logging in tropical forests, only a few studies have focused on using remote sensing to assess this impact. This study aims to utilize remote sensing approaches to assess carbon emissions from selectively logged forests in the production forests of Malaysia. For this, we incorporate automation and machine learning techniques and utilize UAVs and high spatial-resolution imagery. To investigate selective logging's impact on AGB and carbon

stock, it is essential to measure the forest parameters and logging indicators associated with this process. Many researchers have measured the forest parameters and logging indicators via ground inventories in the past [8,22,23]. However, in dense production forests, such as the ones in Malaysia, the integration of both ground and remote sensing approaches is required to enhance the measurement process in terms of time and cost [7]. To the best of our knowledge, this is one of the first studies that extracts and considers all logging impact indicators such as stump height, stump diameter, cross-sectional area, timber volume, logging gaps, road, skid trails, and incidental damage resulting from the logging process in model development, whereas the previous studies in the literature only consider a few of these parameters when developing the model. Moreover, this study attempted to model emissions based on their overall impact instead of focusing on estimating emissions individually.

## 2. Materials and Methods

### *2.1. Study Area*

The study area was conducted at Ulu Jelai Forest Reserve (UJFR), a production forest located in Lipis District, Pahang, Malaysia (Figure 1). The logging operation in UJFR is subjected to the SFM logging policy. The logging activities in this area are supervised by a specific section of the Pahang Forestry Department and the Malaysia Timber Certification Council (MTCC). The whole of the investigated area was in the production forest, and active logging included compartments 124, 159, and 160, which experienced a second cycle of logging operations with approximately 25–30 years cycle intervals. The total area of the compartment was 83 ha, and the flying area of the ground sampling was 48 ha. UJFR experiences a humid climate, the average annual precipitation ranges from 1500 to 2000 mm, and the average surface temperature ranges from 24 to 34 °C [24]. The terrain conditions were hilly, and the terrain landscape of this study area varied from 60 m to 800 m above the mean sea level. The general species of forest trees in the study area were lowland Dipterocarp Forests, with Meranti (*Shorea* spp.) and Keruing *(Dipterocarpus* spp.) as the dominant species. The average height of tall evergreen trees was between 30 m and 50 m height.

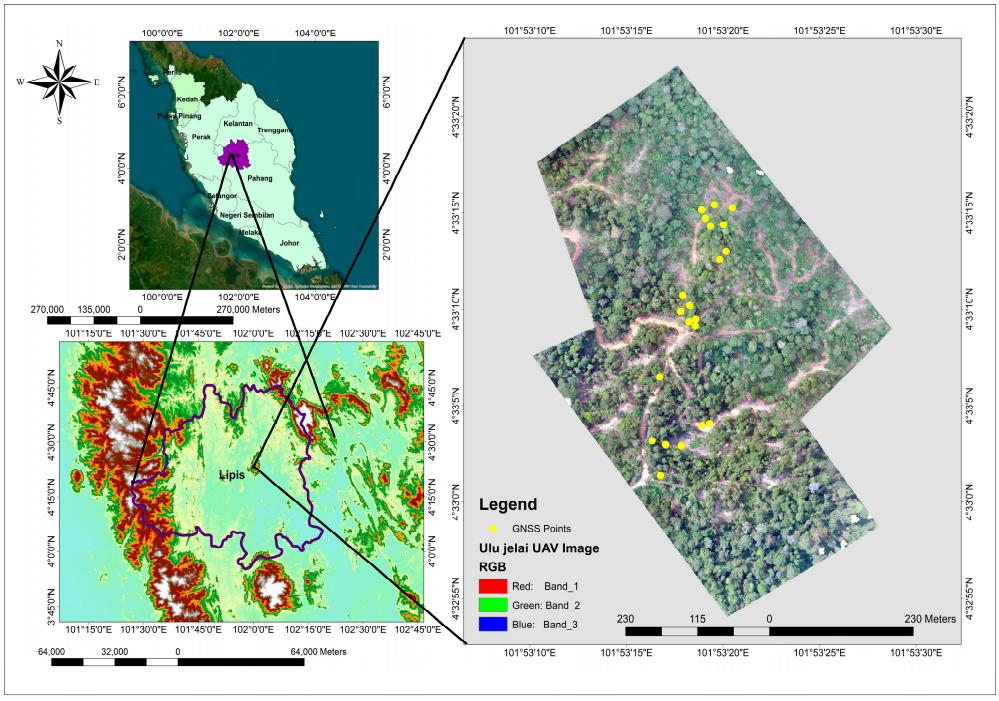


**Figure 1.** Map of the study area (UJFR), Pahang, Malaysia, with a close-up of Lipis District and distribution of sampling points in the research area.

### *2.2. Data Acquisition*

This study involved two sources of data collection: (i) Ground data and (ii) Remote sensing data.

#### 2.2.1. Ground Data Acquisition

Selective logging data were measured on the ground at the study site, UJFR, in the first phase of data collection from 19 August 2019 to 23 August 2019. The purpose of this process was to obtain and make an inventory of selective logging impact parameters that were available on the site. During the data collection process, the diameter tape was used to measure selective logging parameters such as the diameter of the stump, length of the log, height of the stump and buttress, logging infrastructures, and logging damage from fallen trees. Global navigation satellite system (GNSS) (Trimble Geo 7X) equipment was used to record the specific location of the stump (X, Y, Z coordinates). Northing and easting requirements at the time of establishing a fix and the GNSS estimation of the location of the middle of the tree-stump dimensions were accurate to one centimeter. The diameter of the tree stump was calculated by averaging the two cross-sectional diameters, which were measured using a measuring tape. The field data were recorded using a field data sheet based on the field data standard operation procedure (SOP) adopted by [10], Forest Research Institute Malaysia (FRIM), and the Lipis Forestry Department. Additionally, some of the details of logging attributes (branches and length of log section) were obtained through computation after data collection based on inventory data from the site. Data collection and measurements focused on left stumps on the site and the environmental damage induced by the logging process to estimate carbon loss following selective logging. There were 21 sampling plots set up, with 21 stumps left on the site after the timber was removed. In this investigation, the stumps were chosen at random from the middle of the three compartments, including compartments 124, 159, and 160.

The total number of stumps selected in this study adequately covered the major tree species of the forest sites (at least 10 dipterocarps species) [7]. These stumps were tagged by a logging contractor during the timber harvesting process before sampling and measuring. The location of the stumps was determined using GNSS equipment with a precision of $\pm 1$ m. The sample stumps were chosen based on the visibility of the stump, the condition of the stump and timber tree, the topography of the forest landscape, and the area's accessibility. Because most of the logs had been removed before data collection was conducted, the stump and crown of each falling tree were discovered and validated by calculating the angle of the tree fall, species, and the acceptable distance from the stump. This assessment was conducted on-site based on the left log section and branches that were visible to avoid bias and incorrect stump and felled tree selection. The selected incidental trees or felling damage were measured for a tree with a DBH $\geq$ 10 cm, as recommended by [4].

#### 2.2.2. Remote Sensing Data Acquisition

Two main sources of remote sensing data were acquired in this study using aerial and space sensors, namely UAV data and satellite data. Together, these data sets provide a high-resolution aerial and space view of the research site.

Most of the selective logging parameters that were required in this study were derived from UAV processing. A digital aerial photograph (DAP) extracted from a UAV was flown above the study site and involved the middle part of compartments 124, 159, and 160 on 19 August 2019. The UAV sensor and its system were successfully launched from the nearby open space in the forest area and flown over the study area using a DJI Phantom 3 Professional multirotor and was controlled in a semi-automatic mode using Drone Deploy software operated from an Apple iPad Mini from the ground. The flying altitude of the Drone was adjusted from 90 m to 172 m during the flying operation. The study scene was captured with an output of 0.60 m, high spatial resolution with 75% front lap and 85% side lap recorded in 252 raw images. Two satellite images from Sentinel-2 and Planetscope were

used in this study as supplemental data to complement the data needed to construct the variable of selective logging to model carbon emissions in the UJFR and give thorough coverage over the research area. The Sentinel-2 image from the year 2018, with a date of 3 June 2018, was used to represent the area before logging, whereas Planetscope imagery from the year 2019, with a date of 18 May 2019, was used to represent the area after the selective logging activities. Planetscope imagery had a 4 m spatial resolution and four spectral bands, including blue, green, red, and near-infrared (NIR) [25]. Sentinel-2 offered 13 spectral bands at 10 m to 60 m spatial resolution [26]. Only four spectral bands (blue, green, red, and NIR) were employed from the Sentinel-2 image. Data from PlanetScope are an excellent resource for monitoring vegetation. In this study, the Planetscope imagery was resampled to a 10 m resolution following a Sentinel-2 resolution of 10 m to extract the possible variables. Both of these satellite data were also atmospherically and radiometrically corrected in the pre-processing stage.

### 2.3. General Methodology

The workflow of the methodology for this study is divided into four stages: data collection, pre-processing, data processing, and analysis and modeling (see Figure 2). The data were acquired from two sources: ground and remote sensing data. At the data processing stage, the variables of carbon modeling were generated via a remote sensing approach and proceeded with the analysis stage. The analysis stage involved the modeling process and validation to quantify the total carbon emissions. Figure 2 below illustrates the overall methodology adopted in this study.

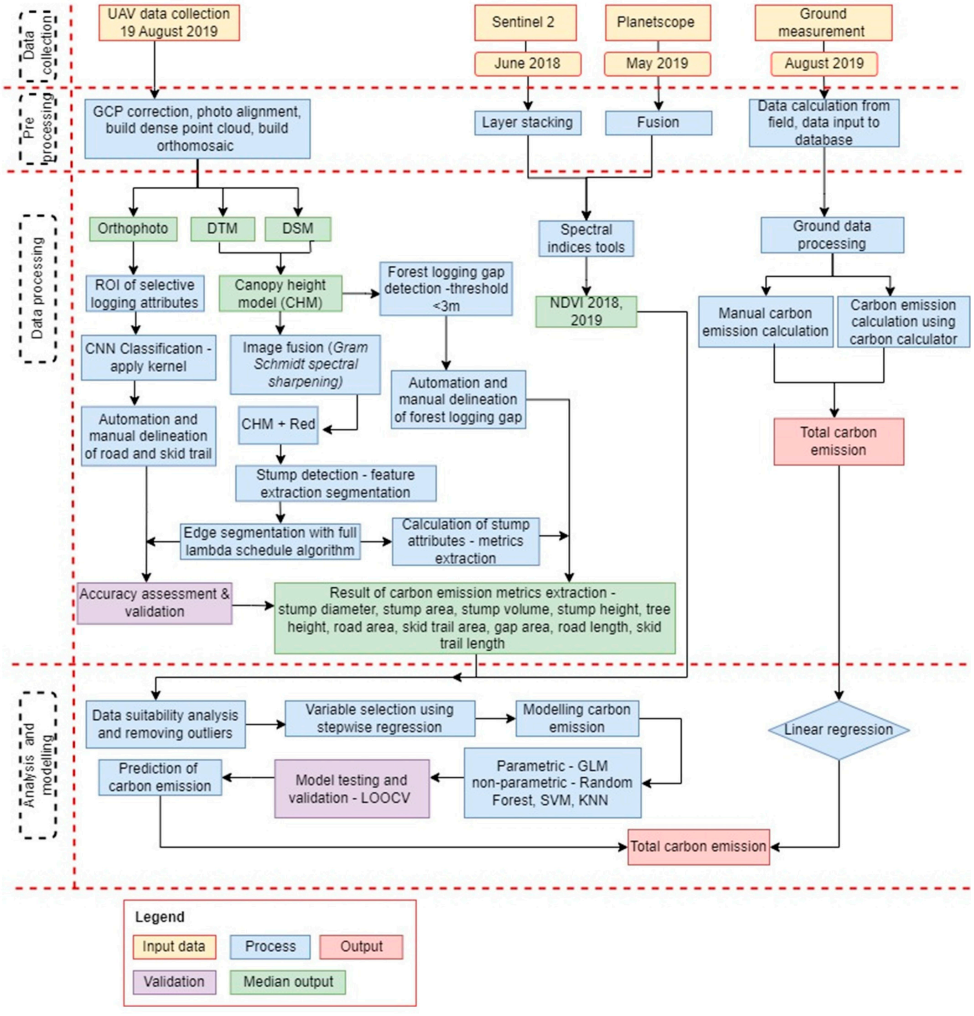


**Figure 2.** Overall workflow of the methodology.

### *2.4. Quantifying Carbon Emissions from Ground Data*

The total carbon emissions from the impact of the selective logging operation were quantified based on the logging parameter that appeared during and after the logging process. A common selective logging impact was identified through the logging indicators appearance, such as the left stumps from timber harvesting, logging infrastructures (haul roads, skid trails, and log yards), and the incidental damage of nearby trees associated with felling timber trees. To quantify carbon emissions from the overall impact of selective logging, the value of emissions from the logging parameter emission sources should be assessed in the first place, followed by summing all the emissions from all sources [27]. The total emissions from the overall impact of selective logging can be formulated through the following Equation (1).

$$\text{Emission from selective logging} = \text{LE} + \text{LD} + \text{LI} \quad (1)$$

LE = logging emission from extracted timber
LD = logging damage from logging process (logging gaps, yard, tree felled)
LI = logging emission from infrastructure (road, skid trail)

The general process of quantifying carbon emissions from ground observation data were solely performed using the Winrock carbon calculator developed by Winrock International, and the calculation was based on above-ground biomass (AGB)'s allometric equation developed by [28] and an improved equation from [29]. The carbon emission was calculated by multiplying the AGB value with the conversion factor based on the Intergovernmental Panel on Climate Change (IPCC) standard.

$$\text{AGB} = 0.0673 \times (\rho D^2 H)^{0.976} \quad (2)$$

$\rho$ = wood density (gm/cm$^2$).

This approach focuses on carbon loss from three main sources of the logging impact (impact from extracted timber, logging gaps, and infrastructure effect). The detailed process can be assessed through findings from previous research [7].

### *2.5. Remote Sensing Data Processing*

#### 2.5.1. UAV-RGB Digital Aerial Photograph (DAP) Processing

The UAV data were processed with Agisoft Metashape Professional 1.5 software to create a DAP or orthophoto with a ground sample distance of 0.60 m. In Agisoft Metashape Professional software, an orthophoto that represented the coverage of the study area was produced based on the workflow available in the software guidelines [30]. The basics related to the generation of the orthomosaic involved the procedure of "align photos", "build a dense point cloud", and "build orthomosaics". A total of 430 million-point clouds were processed to generate the elevation data, which were used to generate a digital terrain model (DTM) and digital surface model (DSM). The canopy height model (CHM) was generated by subtracting the values of DSM and DTM (DSM—DTM). The CHM value is required to calculate the height of the logging impact indicator. Ground data filtering was implemented to remove unwanted terrain heights or non-ground data while processing DTM and DSM. The final output was prepared for the next processing phase to extract the possible variables required in carbon emission modeling.

#### 2.5.2. Satellite Data Processing

Other potential variables that were required in this study were extracted from satellite data. Sentinel-2 and Planetscope were used to extract the normalized difference vegetation index (NDVI) values before and after selective logging took place. NDVI quantifies vegetation using reflected light in the near-infrared and visible bands and determines the density and health of vegetation through each pixel in a satellite image. NDVI is commonly used in vegetation analysis, such as mangroves [31] and forests, and is widely used to predict

carbon stock and carbon emissions [32,33]. NDVI can derive forest attributes in terms of their density and can be used as carbon emission variables for predicting carbon emissions from selective logging activities based on the value of the indices employed from multi-spectral bands in satellite imagery [34]. NDVI was calculated using red and near-infrared channels as in Equation (2), with NDVI values varying from −1 to 1. The selected spectral for the red band is band-3 from Planetscope and band-4 from Sentinel-2 imagery, while the spectral from the near-infrared band is band-4 from Planetscope and band-8 from Sentinel-2 imagery. Therefore, the NDVI output results were generated from ENVI software. Hence, the maps produced were exported and created using ArcGIS software.

$$\text{NDVI} = (\text{NIR} - \text{Red})/(\text{NIR} + \text{Red}) \quad (3)$$

The NDVI values indicate the amount of green vegetation present in the pixel. Higher NDVI values indicated a higher density of green vegetation. Using the spectral indices tool in ENVI 5.2 software, NDVI from Sentinel 2018 and Planetscope 2019 were generated. The NDVI mean values of 21-point locations were extracted and compared from both results. Maps of the carbon stock's spatial distribution and index value were also created. The sample areas were chosen based on the value of the dispersion of the vegetation index. The vegetation index value corresponding to the 21 GNSS points were tabulated, including NDVI 2018, and 2019, the mean value, and the difference in NDVI values between the two years.

### *2.6. Extraction of Varibales/Metrics*

Timber trespass and residuals, forest gaps, and damage from construction logging infrastructures were important indicators for defining logging and selective logging operations in production forests. Consequently, we attempted to identify these significant parameters using a remote sensing approach to the UAV data. A different approach was used to determine other logging parameters, which later were used as possible metrics or variables for modeling carbon emissions.

#### 2.6.1. Tree Stump Detection and Associated Attributes

The structure of the stumps that were left at the logging sites was uniform in shape [17] and had an almost circular appearance with a variety of diameters and heights depending on the age and size of the tree. Theoretically, any round-shaped object visible in the images could be a potential left stump after harvesting. In most of the post-logging inventories, the stumps were identified manually, and the area of the stumps was typically computed using conventional ground measurements, either measuring the longest or shortest distance of the stump and calculating the area of the corresponding circle [18]. Geographic object-based image analysis (GEOBIA) based on feature extraction from the segmentation technique was used for this process to detect stumps since segmentation allowed the detection of the object based on its segmented shape and structure. In this context, the object-based approach enables a good delineation between forest attributes from selective logging (stump) and the extended damage associated with it. Segmentation is the process of partitioning an image into objects by grouping neighboring pixels with common values. The objects in the image ideally correspond to real-world features. Effective segmentation ensures that classification results are more accurate. This study adopted image segmentation based on the Edge segmentation algorithm with the full Lambda schedule algorithm created by [35]. Edge segmentation is a feature extraction process and is effective for segmenting edges and clear object shapes. The merging algorithm (full Lambda schedule) merges adjacent segments iteratively using a combination of spectral and spatial information, and during the process, the merging algorithm finds the pairs region and (e.g., i and j), with the merging cost, t is less than a defined threshold, T. refers to Equations (4) and (5) [36].

$$t_{i,j} = \frac{\frac{|o_i| \times |o_j|}{|o_i| + |o_j|} \times \| u_i - u_j \|^2}{length(\partial(o_i, o_j))} \quad (4)$$

where $o_i$ and $o_j$ are the regions i and j of the image, $|o_i|$ and $|o_j|$ are the areas of regions i and j, $u_i$, and $u_j$ are the average spectral values in the region i and j, $\|u_i - u_j\|$ is the Euclidean distance between the spectral values of region i and j, while the length, $\partial(o_i, o_j)$ is the length of the common boundary of i and j.

$$\text{Lambda} = \left[\frac{N_i \times N_j}{N_i + N_j}\right] \times \frac{E}{L} \quad (5)$$

where $N_i$ and $N_j$ are the numbers of pixels in the region i and j, respectively, $E$ is the Euclidean color distance, and $L$ is the length of the common boundary.

This approach was performed using ENVI Software version 5.2 and completed the refinement with ArcGIS 10.4 (Figure 3), set to appropriate parameters and algorithms (Table 1).

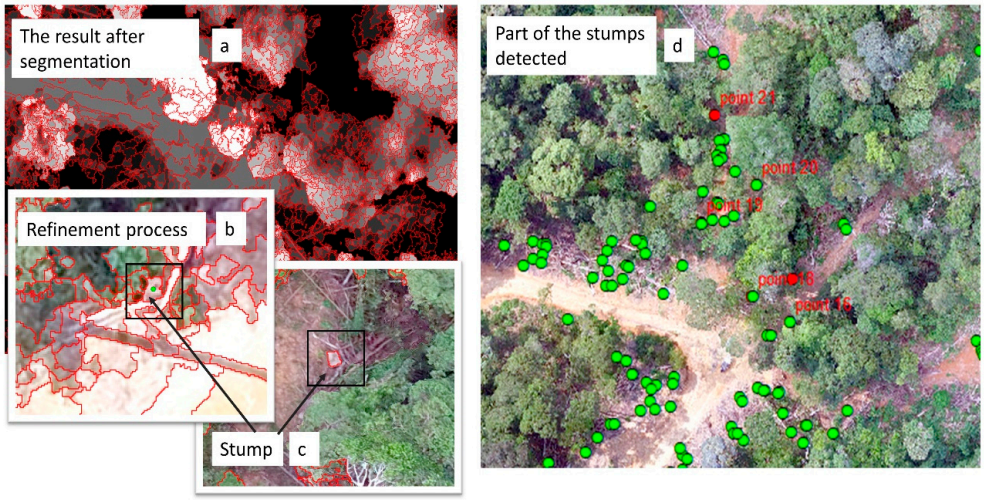


**Figure 3.** The segmented tree stumps, after segmentation (**a**), the refinement process (**b**), identified stumps (**c**), and part of the identified stumps' distribution (**d**).

**Table 1.** Parameters and algorithms for the segmentation process.

| Setting Parameter | Algorithm | Level | Remark |
|---|---|---|---|
| Segment | Edge | 44 | Scale level |
| Merge | Full Lambda Schedule | 21 | Merge level |
| Kernel size | | 3 | |

For the segmentation process, the Edge parameter is useful to identify the edge of features and sharp borders and was set up to a 44-scale level where it met the criteria to effectively delineate objects such as stumps and left logs. During this stage, it was not set for any merging since we wanted to prevent merging with other similar spectral information, such as elevation and other related attributes, which were not necessary for this section. The algorithm used for merging settings after segmentation was the full Lambda schedule with a merging level of approximately 21 after adjusting the output. The image from the generated CHM was fused with the UAV-RGB imagery red band to enhance the stump visibility in the image to achieve a more accurate segmentation result. The merging process combines adjacent segments with similar spectral attributes, and we used the default merging algorithm, which allows a larger object to merge with textured areas. The higher value of the merging scale effectively delineates highly textured features.

Merging combines adjacent segments with similar spectral attributes, and we used the default merging algorithm, which allows for the merging of a larger object and textured areas and distinguishes unnecessary segments that might be a great challenge during the refinement process. The higher value of the merging scale will effectively delineate highly textured features. The default setting for texture kernel size was set to three as it is sufficient for small areas with a variance of object texture. Segmented output was saved as vector-based data and processed in a shape file format with its texture attributes, including its spatial information. These steps allowed the cleaning and refinement process to be performed as a vector-based output.

#### 2.6.2. Stump Structures Derivation for Variable Selection

The structure of the visible stumps left on site after selective logging was measured and can be extracted from the stump's detection process using a UAV. These variables were also collected on the ground when ground inventory was taking place, which had been used to calculate carbon emissions using the Winrock calculator. Each visible stump can be defined by its structures, such as the height of the stump, diameter, area, and volume of the stump. CHM data generated from the UAV could be used to derive the height of stumps that are visible on the image after the stump-detecting process [19]. In this study, the stump height was extracted from CHM fused with a red band, and the stump height was computed by taking the mean elevation of all pixels that represented the stumps visible on the image, and the height value was multiplied by a cross-sectional area of the stump to estimate the volume. To facilitate the visual part of calculating stump structures, the stumps were co-rectified with the positions of the stump on the ground and manually fitted with the detected stump on imagery to best fit its shape and height from CHM. The area and diameter of the stumps were calculated using calculating geometry in ArcGIS Software. The results of these stump structures were verified with measurements on the ground using a simple linear regression model.

#### 2.6.3. Other Logging Indicators—Logging Gaps and Logging Infrastructure

The other logging indicators, in addition to timber tree stumps, were identified to quantify the effect of selective logging on carbon emissions. For this purpose, a machine learning classification was used, and variables or metrics of logging indicators were derived from the output. The convolutional neural networks (CNN) classifier was selected as a machine learning algorithm to extract logging indicators in UAV images that contributed to the impact of selective logging on carbon emissions. There were some studies that had used this technique in the past for object detection analysis but used a computer vision approach. This procedure required training data sets known as the region of interest (ROI), which described all features that appeared to be a logging indicator in the image. ROI was set for tree stumps, logging roads, skid trails, felled logs, bushes, and gaps. By applying this algorithm to the desired training data sets or ROI, the impact of logging indicators was automatically classified.

Different parameter iterations of 500, 700, and 1000 were applied for the same study area (Table 2). This is because the iterative modeling using CNN needs to be tested for its UAV image as well as the mapping of affected areas such as main roads, skid trails, tree stumps, and fallen logs. CNN classification was performed using ENVI 5.2 software. In this study, CNN, with seven layers of hidden nodes and a training rate of 0.2, was considered sufficient to produce an indicator classification output for the impact generated in the selected logging area.

**Table 2.** Training rate and iterations for CNN classification.

| | 1st | 2nd | 3rd |
|---|---|---|---|
| Training Rate | 0.2 | 0.2 | 0.2 |
| No of Iterations | 500 | 700 | 1000 |

Using ArcGIS Desktop 10.4, the result classes in vector format from the machine learning classification were then exported from ENVI 5.2. Hence, all the impact indicator areas in hectares were calculated from the attribute table in ArcGIS 10.4. At this stage, the cleaning and refinement process was performed to refine the classified features and delete the unnecessary classified features with the aid of visual interpretation. The classification output, which are roads, skid trails, and logging gaps, were identified and used as input variables in carbon emissions modeling. This automation feature extraction approach was reliable, and the validation was conducted based on the manual delineation method through image vectorization. The refinement and cleaning process was then conducted to carefully distinguish the variables. At the same time, a manual process (image vectorization) was also adopted to derive the logging attributes, such as roads, skid trail, and logging gap, to verify the accuracy since this process was considered to replace ground observation for this data extraction [11].

Logging gaps and logging damage areas are often a major impact of selective logging; thus, it becomes an essential indicator when assessing carbon loss from selective tree harvesting. This research implemented manual and automation approaches to map the damaged parts. Since the forest gaps always vary with terrain conditions in a particular forest area, gap definition based on the opening forest at a certain elevated ground area could be considered [37,38]. Automation gaps detection apply to CHM data derived from dense point cloud produced in UAV imagery by referring to the definition of gaps in the forest canopy that are similar to [11,20], which define the gaps as damaged area coverage that extends to an average height $\leq$ 2 m above the ground [39] and mostly is below a 3 m height. To obtain this result, a threshold of 3 m was reclassified on CHM data to portray the defined gaps, and this allows the inclusion of the felled tree crown as a logging gap that met the gap's criteria for selective logging impact for this study. The manual delineation of selective logging gaps was also performed by performing image vectorization on vector inputs in ArcGIS software then the output could be used as validation.

### *2.7. Carbon Emission Model Development*

Statistical analysis and modeling were performed in R version 4.1.3 using several statistical packages. Stepwise regression analysis was adopted in this study to evaluate the best subset of potential independent variable combinations in the dataset. Hence, the strength of relationships between carbon emission and variables derived from UAV and satellite data needs to be evaluated since the relationship between forest AGB or carbon emissions with the predictors generally varies with different forest types and conditions [40]. Stepwise regression is a common method for assessing numerical variables in statistics, especially when it involves non-parametric data, and is often used for the identification of variables for carbon modeling [41]. To establish a good model, the nature and suitability of the potential variable should be considered through the test from stepwise regression. The stepwise forward selection was performed, and the variables selection was based on the lowest Akaike information criterion (AIC) and variance inflation factor (VIF). The forward selection starts with a null model with no predictor and proceeds with adding one variable at once, allowing the model to be tested by each variable. The Shapiro–Wilks normality test, also known as the non-parametric normality test, was applied to all potential variables in this study to observe the normality curve of the variable data distribution with the hypothesis that the data were non-normal distributed. Thirteen variables were tested (Table 3), namely, diameter, height, volume, wood density, logging gaps, road, skid, NDVI for the year 2018, NDVI for the year 2019, mean NDVI, and NDVI difference between the year 2018 and 2019 with 21 data entries according to ground data as a validation data. The dependent variable (Y) included carbon emissions derived from the ground, and the independent variables were potential variables mentioned before as (X) factors. These parameters or variables are similar to the data details collected during the ground investigation to make sure the parameter is related and provides acceptable results.

**Table 3.** Metrics derived from the UAV and satellite as independent variables.

| Metrics | Metrics Descriptions |
|---|---|
| Height | Height of stumps |
| Diameter | Diameter of stumps |
| Area | Area of stump based on cross-sectional area coverage |
| Volume | Volume of stump |
| Gaps | Area of logging gaps |
| A road | Area of roads for logging |
| A skid trail | Area of skid trails to transport logs |
| L road | Length of roads for every section |
| L skid trails | Length of skid trail for every section |
| NDVI 18 | The value of INDVI represent by each sample point for the year 2018 |
| NDVI 19 | The value of INDVI represent by each sample point for the year 2019 |
| Mean NDVI | Mean NDVI value between years 2018 and 2019 |
| Diff NDVI | The difference in NDVI values for the years 2018 and 2019 |

Using this regression model, the output was selected based on theAIC, which considers the lowest value as a good subset of variables, and its multicollinearity between dependent and independent variables was also tested based on a VIF greater than five. AIC is the goodness of fit that analyses the favors' small residuals error in the model developed but penalizes the inclusion of predictors, thus, helping in avoiding overfitting, while the VIF was used to address the issue of multicollinearity between the variables by computing and monitoring the size of the condition numbers [42].

For modeling carbon emissions, three machine learning algorithms and a linear model were used to evaluate carbon predictors (independent variables) derived from remote sensing by referring to the reference carbon emission derived from the ground (dependent variable—logged carbon emission). Modeling parts involved (1) model development and (2) model assessment. A total of 21 samples of the data were applied to match the number of sample data collected on the ground over 48 ha of the flying region from UAV.

The algorithm adopted in this study was the support vector machine (SVM), random forest (RF), K-nearest neighbors (KNN), and linear regression model (LM), which were validated using referenced carbon emissions derived from ground data. Leave out one cross-validation (LOOCV) model performance that was used to evaluate the performance of the developed model. This validation technique fits with the number of data used since it is applicable for the small dataset by using all sample data as test data and only one data left out as validation data. Comparisons between the models to find the best model that matched the objective of this study were based on their predictive capabilities, most common indicator root mean square error (RMSE), bias, coefficient of correlation ($R^2$), and adjusted $R^2$ (Adj-$R^2$) [11,41]. A lower RMSE and bias indicated a better regression model, and higher $R^2$ values represented a good model as well with a strong correlation. RMSE and $R^2$ were used as methods to evaluate the measured value and estimate the value [42] and are expressed as follows:

$$\text{RMSE} = \sqrt{\frac{\sum_{i=1}^{n} (yi - \hat{y}i)^2}{n}} \quad (6)$$

$$R^2 = 1 - \frac{\sum_{i=1}^{n} (yi - \hat{y}i)^2}{\sum_{i=1}^{n} (y - \overline{y})^2} \quad (7)$$

where $yi$ is the observed value and $\hat{y}i$ is the predicted value for the $i$th compound, respectively; $n$ is the number of observations in the training sets and $\overline{y}$ is the observed mean value [12].

## 3. Results

### *3.1. Stumps Detection and Its Attributes*

The segmentation result for feature extraction based on the edge algorithm with a full Lambda schedule algorithm expresses a raw output (Figure 3a), as the algorithm detects and segments the possible edge of the boundary for all objects detected on the CHM-fused red band image. Thus, a cleaning and refinement process was needed to reclassify the possible stumps (Figure 3b,c), and the format of data representation was converted to point-vector-based to display the distribution of the overall stumps that had been detected by the algorithm (Figure 3d). The total stumps detected were 473, with 21 of them co-registered with 21 stumps from ground sampling.

### *3.2. Other Selective Logging Impact Indicators (Roads, Skid Trails, and Logging Gaps)*

To assess the accuracy, the number of stumps detected was evaluated based on the omission and commission errors which identified the number of stumps that matched with the stumps measured on the ground across all three logging compartments (Table 4). Overall, 479 stumps were detected across the 48 ha surveyed area with an accuracy of 69.74%. The omission and commission errors reported at compartment 124 were 22.22% and 42.86%, 40.00%, and 66.67% reported for compartment 159, and 28.57% and 40.00% reported for compartment 160. When validating with the field data, it was found that 15 out of 21 ground sampling were detected by this algorithm. This result is considered acceptable since the data captured at a moderate flying altitude with the condition of the stumps on the ground was not well presented in the image due to the stump's conditions and canopy coverage.

A ground–automated validation was conducted using simple linear regression to assess the accuracy of the remote sensing technique in extracting forest logging attributes. The findings of the result are satisfied with an overall value of the coefficient of correlation ($R^2$) as an acceptance indicator shown above 0.5 (Figure 4). This shows that the accuracy of the process is from moderate to good, where it is considered acceptable based on the score of the $R^2$. The height of the stump was able to be detected with moderate accuracy, and it is considered acceptable for this study considering that this research was intended to utilize low-cost data, and most of the stumps were formed by their buttress with a height of more than 1 m.

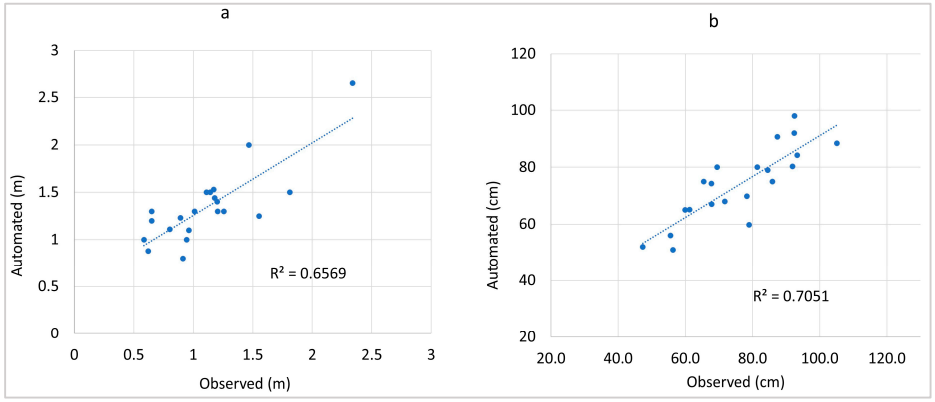


**Figure 4.** The scatterplots of the relationship between UAV predictions and the ground observation of stump height (**a**) and stump diameter (**b**).

### *3.3. Other Selective Logging Impact Indicators (Roads, Skid Trails, and Logging Gaps)*

For the CNN classification, nine regions of interest were selected over the UAV imagery. The total polygons and pixels used were a total of 152 polygons and 38,544 pixels for the training data, as shown in Table 4. Nine regions of interest comprised stumps, roads, skid trails, fell logs, felling trunks, forests, cars, dead trees, and no pixels. The fill, orien, and space parameters remained the default value. In this study, CNN with one layer of hidden

nodes failed to show the output of the classification; therefore, CNN with seven hidden nodes and iterations of 500 were selected to perform a CNN classification (Figure 5). Three types of iterations have been compared to the performance of each CNN classification method, iterations 500, iterations 700, and iterations 1000. Under all three CNN iterations, iterations of 500 shows the best performance with an overall accuracy of 78.564% and a Kappa Coefficient of 0.6977.

**Table 4.** Parameters used in CNN classification.

| ROI Name | Pixels | Polygons | Fill | Orien | Space |
|---|---|---|---|---|---|
| Stumps | 1105 | 24 | Solid | 45 | 0.10 |
| Road | 38.926 | 20 | Solid | 45 | 0.10 |
| Skid Trail | 10,440 | 15 | Solid | 45 | 0.10 |
| Fell Log | 2846 | 46 | Solid | 45 | 0.10 |
| Felling Trunk | 2180 | 18 | Solid | 45 | 0.10 |
| Forest | 13,938 | 16 | Solid | 45 | 0.10 |
| Car | 511 | 3 | Solid | 45 | 0.10 |
| Dead Trees | 597 | 8 | Solid | 45 | 0.10 |
| No Pixel | 6888 | 2 | Solid | 45 | 0.10 |
| Total | 38,544 | 152 | | | |

Other selective logging indicators that were identified to be evaluated as carbon model variable parameters were the logging infrastructure (logging roads, skid trails), and damaging impacts included logging gaps and a temporary log yard. These gaps are considered a wide gap since the development of the log yard leaves out a huge opening of forest area. Through image classification and threshold re-classification, the variables can be identified and presented in area and length (Figure 5). The total length of the logging roads was 2391.514 m, with 2.349 ha identified. The skid trail was classified as 2680.875 m in total length, and the area was calculated to be 1.553 ha. The total area of logging gaps that were considered damaged impact from the logging, including the log yard, was 7.44 ha.

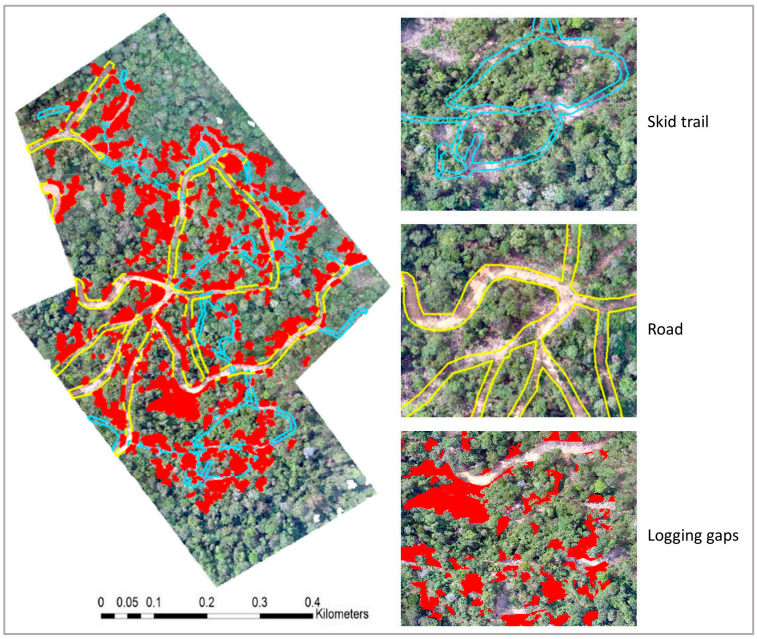


**Figure 5.** Roads, skid trails, and logging gaps identified as logging indicators.

NDVI values for the study area were extracted from two satellite images before and after the logging operations took place. The indices values were derived from the NDVI methods using the Sentinel year 2018 and Planetscope year 2019 over the Ulu Jelai forest

reserved area. The NDVI resulted from Sentinel 2018 images ranging from 0.51 to 0.71. By looking at the results in 2018, nearly all the study regions were still covered in vegetation. This is due to the imagery captured before the selective logging activities, dated 3 June 2018. While the Planetscope image was acquired in 2019 after the selective logging operations performed in December 2018, NDVI values are significantly lower than the NDVI value from the 2018 image, which has a minimum value of 0.136 and a maximum value of 0.969. The NDVI value distribution of both image displays is shown in Figure 6 The values were extracted from the 21 plots. The difference was then calculated to represent the changes in forest density to be used as potential forest parameters in carbon emission modeling. The average value of NDVI for both years 2018 and 2019 were 0.637 and 0.315, respectively.

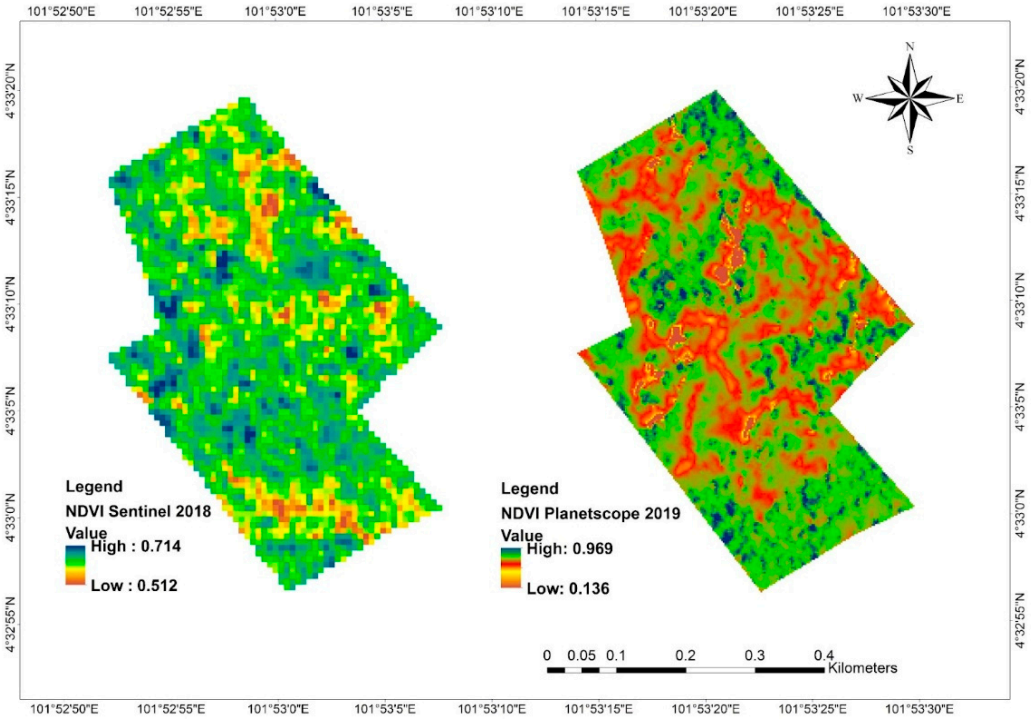


**Figure 6.** NDVI map between the years 2018 and 2019.

### *3.4. Carbon Emission from Selective Logging's Impact*

From the process, the area of the logging gap, area, and length of the logging roads was the best potential dependent variables which are stated in Table 3. Other derived variables, as mentioned in Table 3 from the previous process, were found to be insignificant after being screened by the variable selection process and were omitted. The potential selected variables then proceeded to model carbon emission. Four models were successfully developed, and the results were plotted to show the distributions of variables between the observed and predicted carbon emissions (Figure 7). The results of selective logging carbon emission estimation using SVM, RF, KNN, and LM models based on UAV and satellite metrics are tabulated in Table 5. For non-parametric models with machine learning approaches, the highest goodness of fit was found to be the SVM model with an RMSE of 21.10%, a bias of −0.23%, and adj-$R^2$ equal to 0.8, followed by the KNN model (RMSE = 24.63%, bias = −9.29, Adj-$R^2$ = 0.75) and RF model (RMSE = 26.93%, bias = −0.20, Adj-$R^2$ = 0.66). For the parametric model, the linear model reveals an RMSE value of 22.14% with 0.72 bias, and Adj-$R^2$ is 0.75, which also shows a reliable result. These findings indicate that the best model that can estimate carbon emission from selective logging's impact is the SVM model. The independent variables that had been identified before showed a strong relationship between observed and predicted carbon emissions according to their $R^2$ value. Based on the best model, SVM, the total predicted carbon emission after selective logging operations in the Ulu Jelai Forest Reserve, Pahang, Malaysia, was 1102.86 Mg C per hectare which con-

sidered the emissions from the overall impact of selective logging, such as tree extraction, and damage from the logging roads, skid trails, and logging gaps.

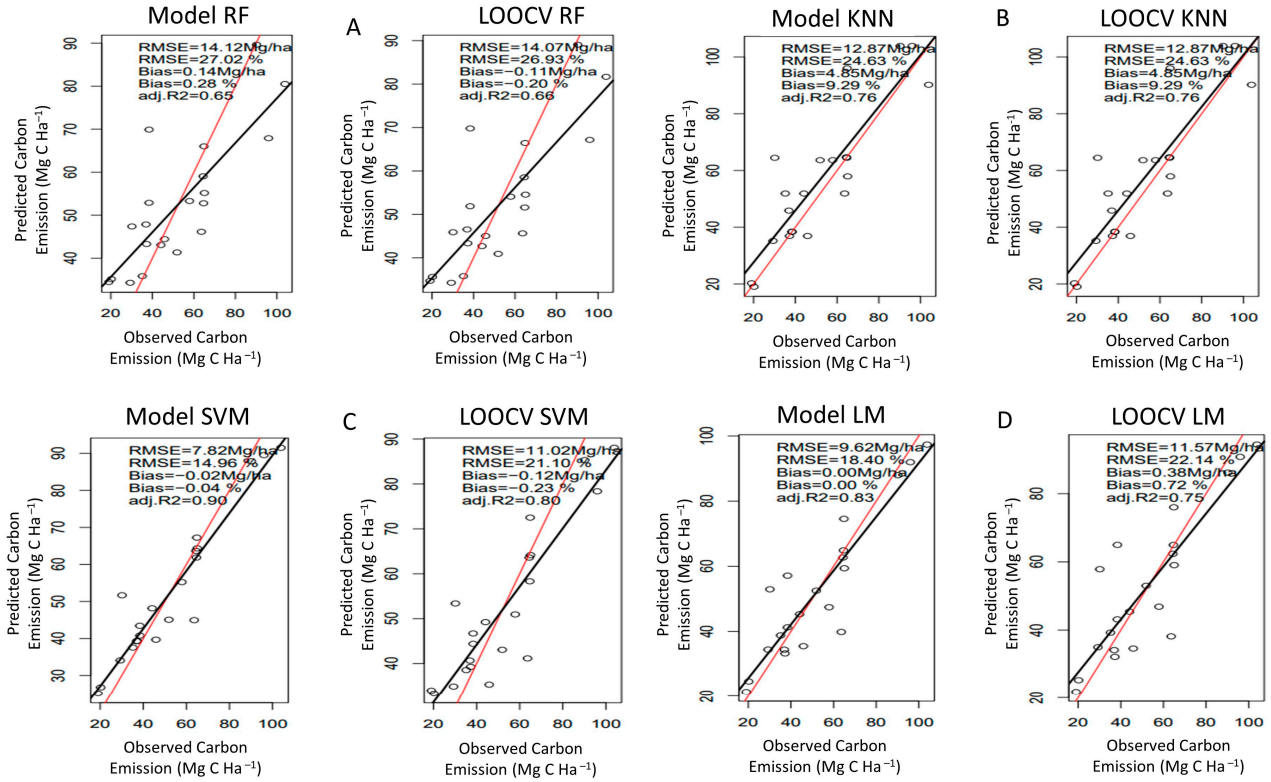


**Figure 7.** Plots of carbon emission models; RF (**A**), KNN (**B**), SVM (**C**), and LM (**D**).

**Table 5.** Training and validation results of the carbon emission model.

| Carbon Emission Model | Training Dataset | | | Validation Dataset | | |
|---|---|---|---|---|---|---|
| | RMSE (%) | Bias (%) | Adj-$R^2$ | RMSE (%) | Bias (%) | Adj-$R^2$ |
| SVM | 14.96 | −0.04 | 0.90 | 21.10 | −0.23 | 0.80 |
| RF | 27.02 | 0.28 | 0.65 | 26.93 | −0.20 | 0.66 |
| KNN | 24.63 | 9.29 | 0.76 | 24.63 | 9.29 | 0.76 |
| LM | 18.4 | 0.0 | 0.83 | 22.14 | 0.72 | 0.75 |

## 4. Discussion

The capability of remotely sensed data to identify forest selective logging indicators such as stumps attributes, damage from logging impacts, and damage from infrastructure construction should be taken into consideration to achieve a satisfactory remote sensing and object-based approach for modeling carbon emissions. Using segmentation methods as part of GEOBIA with a full lambda schedule algorithm to identify stumps as a potential variable is considered successful since it can successfully detect stumps that vary from 0.5 m to 1.5 m in diameter size with a moderate accuracy of approximately 70%. There are limited numbers of research intended to detect the stumps' post-selective logging, especially post-selective logging; hence, a limited comparison could be made.

Several studies involved applying automation techniques for stump detection but focused on a clear-cut forest; therefore, the accuracy and approach might differ from ours. A different segmentation approach by [21] in a similar study area used the integration of a multiresolution segmentation algorithm and template matching. The reported moderate accuracy included 70% of stumps being detected and 80% accuracy for image classification. This range of accuracy (70–80%) is considered common in this kind of study event with different approaches applied to UAV imagery, such as using segmentation integrated

with machine learning classifications in automatically detecting stumps after logging as applied by [17] and since the studies focused on clear cut tree harvesting, which is more clearly visible on UAV images, the stump with the smallest diameter was easily detected with higher accuracy. Ref. [18] generated approximately 77.3% accuracy when detecting loblolly pine stumps using a small UAV with an image pattern recognition algorithm. The accuracy result obtained from our study was comparable with the findings from [20,21], with omission errors of 22.22% and commission errors ranging from 40.00% to 60.00%, which is probably due to the use of a similar study site and an almost similar approach. Nevertheless, both the omission and the commission error obtained by [18] were slightly lower than those found in our study, which ranged from 16.30% to 20.4% and 12.8% to 79.50%, respectively, probably due to a different segmentation algorithm, the sensor used, and the nature of the study area. Meanwhile, the study from [17] resulted in the same range of omission errors (20.00% to 32.1%); however, the commission error is slightly lower, as well as the percentage of accuracy ranging from 26.00% to 34.7%. The variation in this omission and commission error might be due to the severity of the discoloration of the stump and its visibility since the image was taken at a higher altitude, and some objects might be wrongly identified using this segmentation algorithm which is of a similar nature in the shape of other logging residues with the tree stumps.

Common ground methods to assess the extracted carbon when the timber tree fell require the forester to analyze the condition of the stumps and their attributes. As an alternative, automation methods using UAV data could be utilized to identify the stumps in the first place. As used in earlier research relating to stump detection, the area and volume could be approximated from information such as the height and diameter of the stumps [17,18]. By detecting the stumps, the measurement of their structures can be estimated. With a promising correspondence volume of the stump and log segments with $R^2$ of 0.70 to those measured in the field, compared to ours (0.610) and which suggested the possibility of the obtained good measurements of stump attributes, Ref. [19] estimated the volume of the stumps and logged debris and its cross-sectional area using the convolutional neural network (CNN) as an automated object detection method. According to the automatic method used in this work, the average diameter and height of the detected stumps were relatively similar to measurements taken from the ground, with an $R^2$ correlation value ranging from 0.5 to 0.8.

The process of the imagery-based automatic detection method requires minimal time spent on the ground and less fieldwork inventory. The capability of UAVs to collect massive data with minimal time spent could be a good help in UAV imagery estimates for larger study scales of post-logging. An automated algorithm such as remote sensing segmentation could offer promising accuracy and effectively detect stumps with a range of precision accuracy from 70% to 80% [19], and the technique could also play an important role depending on the data image visibility. To improve these results, it is necessary to obtain the imagery at a lower altitude with fewer obstacles and implement advanced automatic algorithms such as CNN. In this study, the detection was performed at a selective logging area with a slightly lower accuracy but still within the acceptable range. This is due to the dense forest canopy cover; hence, the limited visibility of the stump's appearance and the UAV image was taken six months after the logging activities were conducted.

To assess other selective logging impact indicators, machine learning classification is also a reliable option. With CNN classification adopted using ENVI software, the attribute of selective logging could be mapped for a general overview, and then further analysis would be needed to enhance the main indicator, such as logging gaps, roads, and skid trails. Ref. [20] evaluated two machine learning approaches, the convolutional neural network (ANN) and conventional-based classification, to map selective logging in the Ulu Jelai Forest Reserve. Their findings found that neural network classifications gave the best accuracy, with an overall accuracy of 78.56% compared to the conventional-based classification. Their findings found that SVM provided the best accuracy, with an overall accuracy of 87.40% compared to the neural network-based (CNN) approach adopted in

this study (78.56%). Based on previous studies [20,43,44], machine learning classification is comparable in accuracy, and this slight difference may be due to the number of iterations and parameters used for performing the classification that is suitable for forest and land classification. The details of the skid trails and logging gaps were important, and this study discovered the potential digital aerial photo derived by UAV to delineate the said parameters. The automation of roads, skid trails, and logging gaps was validated by the manual delineation technique and image vectorization from UAV imagery and was compared to the measurement made on the ground. The previous study applied on-screen digitization comparable to ours and found it acceptable with good precision, as found by [11,27]. This study's results reported 2391.514 m and 2680.874 m haul roads and skid trails, respectively. Another study, by [45], discovered that haul roads and skid trails from this delineation technique resulted in 71 km and 657.2 km, respectively. Due to the extent of the study region, this is distinct in terms of length, which shows the efficacy of the applied approaches.

There are limited studies that specifically investigate modeling selective logging's carbon impact based on remote sensing data; consequently, the number of studies that can be compared to the findings of this study, especially in Malaysia, is limited. Hence, the analysis of findings referred to conventional selective logging impact in another region of tropical forest and AGB and carbon modeling from individual trees using similar approaches. On ground estimation, the carbon impact from selective logging is more likely to be influenced by the damage from selective logging and the construction of logging infrastructures. Undoubtedly, during the tree harvesting process, many trees are extracted for construction and leave massive logging gaps that affect the unnecessary carbon loss. Thus, for modeling carbon using logging variables derived from remote sensing-UAV data, logging damage-related variables seem to have a big influence by analyzing the findings from the variable selection procedure. Logging roads and logging gaps become the main influenced variables that contributed to the loss of carbon in the selective logging compartment for this study. This is supported by [27], which found tree extraction, residual damage, logging infrastructures, the construction of roads and skid trail, and logging damage such as logging gaps and log yards to contribute to 59% of AGB from the selective logging practice in their study area. Ref. [3] conducted similar studies to study the changes in AGB before and after selective logging using digital aerial imagery from UAVs, which focused on felling trees and found that instead of felled trees, residual damage and logging infrastructure also played an important role in emitting logging-sourced carbon. The study from [45] provides comparable results with our study, only that their study was conducted by utilizing airborne LiDAR data over the Borneo's Forest area. Logging gaps were automatically classified in detail based on the average elevation height with the threshold below 3 m. This allowed the inclusion of tree crowns to be defined as gaps. Ref. [11] decided that the forest gaps were in the range of 0 to 3 m in height, and the gap should be 20 $m^2$ in area. The total area of logging gaps from this study is 7.44 ha, including all canopy gaps and the log yard. In our study, we did not separate temporary log yards from other logging indicators since the construction of the log yards was fewer, and the nature of the impact was the same as logging gaps from the extracted tree.

Before proceeding with the models, it is important to evaluate the logging parameters that are most highly correlated to the value from references to carbon emission. The analysis involved all potential predictor variables extracted from the remote sensing procedure based on the AIC and VIF value produced from stepwise regression analysis as performed in several types of research such as [42,46], Many studies found that machine learning techniques, especially in estimating carbon emissions for tropical forest trees, had the performance accuracy of RMSE in a range of 15% to 20% [11,42] with an average $R^2$ value below 0.8, which shows a decent result of the machine learning technique. The findings from this study produce a slightly higher RMSE value, with most of the models showing a range from 20% to 30%, but the range of $R^2$ was almost similar, and bias was also acceptable and comparable. Our model has a limited number of observations and covers a smaller

research area due to the constraint of data collection over production forests. Among several machine learning models, RF and SVM are commonly used and produce good accuracy in modeling AGB and carbon [40], and RF was found to be the best model [40,46]. The overall accuracy of our approach, starting from the identification of suitable variables or predictors which represented the selective logging indicator, might be due to the period of data taken from the actual date of logging, the altitude of the flying height, and sensor types that are not as precise as the one used in LiDAR and the forest conditions that limit the number of samples to be taken. Nevertheless, the overall result is reliable even though, in some parts, the accuracy was slightly lower than in other similar research. In terms of deriving the logging attributes which involved the information of the terrain heights, integration with other sources of more accurate elevation data such as DTM or DSM was highly recommended, such as integrating with the terrain elevation derived from LIDAR [47], terrestrial laser scanner (TLS) or using elevation data from other methods such as leveling and geodetic measurement as provided by the related agency such as The Department of Survey and Mapping, Malaysia. In addition to that, it is suggested to increase the number of observations on the ground as a reference and utilize data using the most accurate devices alongside looking forward to automation techniques that are more advanced and sophisticated, such as deep learning classification, e.g., computer vision algorithms such as the regional-based convolutional neural network, (R-CNN), faster R-CNN, etc. Certainly, this technique should be evaluated since it is hard to be applied to complicated logging forest regions such as this study area. As for modeling, a wider study area must be considered making the model more reliable and applicable in other regions. The evaluation of numbers of different machine learning models, such as linear-based learners, kernel-based models, and tree-based models, can also have potential. Throughout the study analysis, remote sensing was found to be a valuable and dependable data source, and analysis techniques were agreed upon by most scientific researchers who actively participated in selective logging impact analysis [3,48,49].

## 5. Conclusions

The analysis from this study demonstrates that metrics derived from digital aerial photography (from UAVs)—to represent selective logging indicators—can be used to develop cost-effective carbon impact from the logging activities of production forests. Low-cost UAVs and multispectral satellite imagery offer moderate to good accuracy and are considered to be a reliable and valid source of data, considering the limitation of the sensors, location, terrain landscape, and topographic condition. Assessing carbon emissions from selective logging practices in commercial logging compartments in production forests in Malaysia is significant since Malaysia depends on the timber industry to generate its gross national product (GNP). Unmanaged logging that results in significant carbon loss will affect the 12th Malaysia Plan towards the 2030 agenda for sustainable development, which was listed in Malaysia's pledges to sustainable development goals (SDG) to combat climate change. This is in line with the UN's SDGs goal 15, which is to protect, restore, and promote the sustainable use of terrestrial ecosystems, sustainably manage forests to combat desertification, and halt and reverse land degradation and halt biodiversity loss. Adopting our proposed approach to a larger area could aim in the development of a monitoring tool to quantify the effect of selective logging in the production of forest carbon stocks at a national and regional scale, therefore, pushing toward developing and achieving SDG.

**Author Contributions:** All the authors have made a substantial contribution toward the successful completion of this manuscript. Conceptualization, S.N.M.S., W.S.W.M.J., K.N.A.M. and H.O.; methodology, S.N.M.S., W.S.W.M.J., K.N.A.M. and A.M.M.K.; software, S.N.M.S., A.M.M.K. and N.M.G.; validation, S.N.M.S., W.S.W.M.J., K.N.A.M., H.O. and M.M.; formal analysis, S.N.M.S., W.S.W.M.J., K.N.A.M., H.O., A.M.M.K. and E.A.; investigation, S.N.M.S., W.S.W.M.J. and K.N.A.M.; resources, A.M.M.K., H.O. and N.M.G.; data curation, S.N.M.S.; writing—original draft preparation, S.N.M.S. and A.M.M.K.; writing—review and editing, S.N.M.S., W.S.W.M.J., K.N.A.M., A.M.M.K., E.A. and M.M.; visualisation, S.N.M.S., W.S.W.M.J., A.M.M.K., N.M.G., E.A. and M.M.; supervision,

W.S.W.M.J., K.N.A.M. and H.O.; project administration, S.N.M.S. All authors have read and agreed to the published version of the manuscript.

**Funding:** The authors gratefully acknowledge the funding for this research work which was under Dana Impak Perdana with grant no: DIP-2018-030.

**Acknowledgments:** We would like to express our gratitude to the Forest Research Institute Malaysia (FRIM), the Pahang Forestry Department and Earth Observation Centre, and the Institute of Climate Change, Universiti Kebangsaan Malaysia (UKM) for providing fieldwork equipment and secondary data.

**Conflicts of Interest:** The authors declare no conflict of interest.

## References

1. Wan Mohd Jaafar, W.S.; Said, N.F.S.; Abdul Maulud, K.N.; Uning, R.; Latif, M.T.; Muhmad Kamarulzaman, A.M.; Mohan, M.; Pradhan, B.; Saad, S.N.M.; Broadbent, E.N.; et al. Carbon emissions from oil palm induced forest and peatland conversion in Sabah and Sarawak. *Malays. For.* **2020**, *11*, 1285. [CrossRef]
2. Pearson, T.R.H.; Brown, S.; Murray, L.; Sidman, G. Greenhouse gas emissions from tropical forest degradation: An underestimated source. *Carbon Balance Manag.* **2017**, *12*, 3. [CrossRef]
3. Ota, T.; Ahmed, O.S.; Minn, S.T.; Khai, T.C.; Mizoue, N.; Yoshida, S. Estimating selective logging impacts on aboveground biomass in tropical forests using digital aerial photography obtained before and after a logging event from an unmanned aerial vehicle. *For. Ecol. Manag.* **2019**, *433*, 162–169. [CrossRef]
4. Ellis, E.A.; Montero, S.A.; Gómez, I.U.H.; Montero, J.A.R.; Ellis, P.W.; Rodríguez-Ward, D.; Reyes, P.B.; Putz, F.E. Reduced-impact logging practices reduce forest disturbance and carbon emissions in community managed forests on the Yucatán Peninsula, Mexico. *For. Ecol. Manag.* **2019**, *437*, 396–410. [CrossRef]
5. de Andrade, R.B.; Balch, J.K.; Parsons, A.L.; Armenteras, D.; Roman-Cuesta, R.M.; Bulkan, J. Scenarios in tropical forest degradation: Carbon stock trajectories for REDD+. *Carbon Balance Manag.* **2017**, *12*, 6. [CrossRef]
6. *National REDD Plus Strategy*; NRE: Putrajaya, Malaysia, 2019; ISBN 978-967-0250-28-1.
7. Siti-Nor-Maizah, S.; Wan-Shafrina, W.M.J.; Khairul-Nizam, A.M.; Aisyah-Marliza, M.K.; Hamdan, O. Determination of Emission Factor from Logging Operations in Ulu Jelai Forest Reserve, Pahang using the Integration of UAV and High-Resolution Imageries. *J. Trop. For. Sci.* **2022**, *34*, 247–257. [CrossRef]
8. Azian, M.; Nizam, M.; Samsudin, M.; Ismail, P.; Nur-Hajar, Z.; Lim, K.; Yusoff, M. Carbon Emission Assessment from Different Logging Activities in Production Forest of Pahang, Malaysia. *J. Trop. For. Sci.* **2019**, *31*, 304–311. [CrossRef]
9. FAO. *Global Forest Resources Assessment 2020: Report: Malaysia*; FAO: Rome, Italy, 2020.
10. Walker, S.M.; Pearson, T.R.H.; Casarim, F.M.; Harris, N.; Petrova, S.; Grais, A.; Swails, E.; Netzer, M.; Goslee, K.M.; Brown, S. Standard Operating Procedures for Terrestrial Carbon Measurement Version 2012. Winrock Int. 2012. Available online: http://www.winrock.org/ecosystems (accessed on 30 August 2019).
11. d'Oliveira, M.V.N.; Figueiredo, E.O.; de Almeida, D.R.A.; Oliveira, L.C.; Silva, C.A.; Nelson, B.W.; da Cunha, R.M.; Papa, D.D.A.; Stark, S.C.; Valbuena, R. Impacts of Selective Logging on Amazon Forest Canopy Structure and Biomass with a LiDAR and Photogrammetric Survey Sequence. *For. Ecol. Manag.* **2021**, *500*, 119648. [CrossRef]
12. Jaafar, W.S.W.M.; Maulud, K.N.A.; Kamarulzaman, A.M.M.; Raihan, A.; Sah, S.; Ahmad, A.; Saad, S.N.M.; Azmi, A.T.M.; Syukri, N.K.A.J.; Khan, W.R. The Influence of Deforestation on Land Surface Temperature—A Case Study of Perak and Kedah, Malaysia. *Forests* **2020**, *11*, 670. [CrossRef]
13. Mohan, M.; Silva, C.A.; Klauberg, C.; Jat, P.; Catts, G.; Cardil, A.; Hudak, A.T.; Dia, M. Individual Tree Detection from Unmanned Aerial Vehicle (UAV) Derived Canopy Height Model in an Open Canopy Mixed Conifer Forest. *Forests* **2017**, *8*, 340. [CrossRef]
14. Mohan, M.; Richardson, G.; Gopan, G.; Aghai, M.M.; Bajaj, S.; Galgamuwa, G.P.; Vastaranta, M.; Arachchige, P.S.P.; Amorós, L.; Corte, A.P.D.; et al. UAV-Supported Forest Regeneration: Current Trends, Challenges, and Implications. *Remote Sens.* **2021**, *13*, 1–30. [CrossRef]
15. Ab Rahman, A.; Maulud, K.N.A.; Mohd, F.A.; Jaafar, O.; Tahar, K.N. Volumetric calculation using low cost unmanned aerial vehicle (UAV) approach. *IOP Conf. Ser. Mater. Sci. Eng.* **2017**, *270*, 012032. [CrossRef]
16. Saad, S.N.M.; Maulud, K.N.A.; Jaafar, W.S.W.M.; Kamarulzaman, A.M.M.; Omar, H. Tree Stump Height Estimation Using Canopy Height Model at Tropical Forest in Ulu Jelai Forest Reserve, Pahang, Malaysia. *IOP Conf. Ser. Earth Environ. Sci.* **2020**, *540*. [CrossRef]
17. Puliti, S.; Talbot, B.; Astrup, R. Tree-Stump Detection, Segmentation, Classification, and Measurement Using Unmanned Aerial Vehicle (UAV) Imagery. *Forests* **2018**, *9*, 102. [CrossRef]
18. Samiappan, S.; Turnage, G.; McCraine, C.; Skidmore, J.; Hathcock, L.; Moorhead, R. Post-Logging Estimation of Loblolly Pine (Pinus taeda) Stump Size, Area and Population Using Imagery from a Small Unmanned Aerial System. *Drones* **2017**, *1*, 4. [CrossRef]
19. Windrim, L.; Bryson, M.; McLean, M.; Randle, J.; Stone, C. Automated Mapping of Woody Debris over Harvested Forest Plantations Using UAVs, High-Resolution Imagery, and Machine Learning. *Remote Sens.* **2019**, *11*, 733. [CrossRef]

20. Kamarulzaman, A.M.M.; Jaafar, W.S.W.M.; Maulud, K.N.A.; Saad, S.N.M.; Omar, H.; Mohan, M. Integrated Segmentation Approach with Machine Learning Classifier in Detecting and Mapping Post Selective Logging Impacts Using UAV Imagery. *Forests* **2022**, *13*, 48. [CrossRef]
21. Kamarulzaman, A.M.M.; Jaafar, W.S.W.M.; Saad, S.N.M.; Omar, H.; Mahmud, M.R. An object-based approach to detect tree stumps in a selective logging area using Unmanned Aerial Vehicle imagery. *Malays. J. Soc. Space* **2021**, *17*. [CrossRef]
22. Mashor, M.J.; Jupiri, T.; Nizam, M.S.; Ismail, P. Impact of Harvesting Methods on Biomass and Carbon Stock in Production Forest of Sabah, Malaysia. *J. Adv. Manag. Res.* **2017**, *5*, 272–288.
23. Putz, F.E.; Zuidema, P.A.; Pinard, M.A.; Boot, R.G.A.; Sayer, J.A.; Sheil, D.; Sist, P.; Vanclay, J.K. Improved Tropical Forest Management for Carbon Retention. *PloS Biol.* **2008**, *6*, 296–303. [CrossRef] [PubMed]
24. Malaysian Meteorology Department (MET). Annual Report of Malaysian Meteorological 2019. Available online: https://m.met.gov.my/penerbitan/laporantahunan (accessed on 20 November 2021).
25. Planet Team. *Planet Imagery Product Specifications*; Planet Labs Inc.: San Francisco, CA, USA, 2021; pp. 1–100.
26. ESA Sentinel Online. Missions, SENTINEL 2. Available online: https://sentinel.esa.int/web/sentinel/missions/sentinel-2 (accessed on 19 November 2019).
27. Neba, S.G.; Kanninen, M.; Atyi, R.E.; Sonwa, D.J. Assessment and prediction of above-ground biomass in selectively logged forest concessions using field measurements and remote sensing data: Case study in South East Cameroon. *For. Ecol. Manag.* **2014**, *329*, 177–185. [CrossRef]
28. Chave, J.; Andalo, C.; Brown, S.; Cairns, M.A.; Chambers, J.Q.; Eamus, D.; Fölster, H.; Fromard, F.; Higuchi, N.; Kira, T.; et al. Tree allometry and improved estimation of carbon stocks and balance in tropical forests. *Oecologia* **2005**, *145*, 87–99. [CrossRef]
29. Chave, J.; Réjou-Méchain, M.; Búrquez, A.; Chidumayo, E.; Colgan, M.S.; Delitti, W.B.; Duque, A.; Eid, T.; Fearnside, P.M.; Goodman, R.C.; et al. Improved allometric models to estimate the aboveground biomass of tropical trees. *Glob. Chang. Biol.* **2014**, *20*, 3177–3190. [CrossRef]
30. Agisoft. *Orthomosaic & DEM Generation (without GCPs)-Help Desk Portal*; Agisoft Metashape Profession Edition; Agisoft: St. Petersburg, Russia, 2021.
31. Bindu, G.; Rajan, P.; Jishnu, E.; Joseph, K.A. Carbon stock assessment of mangroves using remote sensing and geographic information system. *Egypt. J. Remote Sens. Space Sci.* **2018**, *23*, 1–9. [CrossRef]
32. Situmorang, J.P.; Sugianto, S. Estimation of Carbon Stock Stands using EVI and NDVI Vegetation Index in Production Forest of Lembah Seulawah Sub-District, Aceh Indonesia. *Aceh Int. J. Sci. Technol.* **2016**, *5*, 126–139. [CrossRef]
33. Gara, T.W.; Murwira, A.; Ndaimani, H. Predicting forest carbon stocks from high resolution satellite data in dry forests of Zimbabwe: Exploring the effect of the red-edge band in forest carbon stocks estimation. *Geocarto Int.* **2016**, *31*, 176–192. [CrossRef]
34. Pacheco-Angulo, C.; Plata-Rocha, W.; Serrano, J.; Vilanova, E.; Monjardin-Armenta, S.; González, A.; Camargo, C. A Low-Cost and Robust Landsat-Based Approach to Study Forest Degradation and Carbon Emissions from Selective Logging in the Venezuelan Amazon. *Remote Sens.* **2021**, *13*, 1435. [CrossRef]
35. Robinson, D.J.; Redding, N.J.; Crisp, D.J. Implementation of a Fast Algorithm for Segmenting SAR Imagery: Technical Report; DSTO-TR-1242 2002.
36. Wang, J.; Jiang, L.; Wang, Y.; Qi, Q. An Improved Hybrid Segmentation Method for Remote Sensing Images. *ISPRS Int. J. Geo-Inf.* **2019**, *8*, 1–23. [CrossRef]
37. Zielewska-Büttner, K.; Adler, P.; Ehmann, M.; Braunisch, V. Automated Detection of Forest Gaps in Spruce Dominated Stands Using Canopy Height Models Derived from Stereo Aerial Imagery. *Remote Sens.* **2016**, *8*, 175. [CrossRef]
38. Brokaw, N.V.L.; Scheiner, S.M. Species Composition in Gaps and Structure of a Tropical Forest. *Ecology* **1989**, *70*, 538–541. [CrossRef]
39. Asner, G.P.; Kellner, J.R.; Kennedy-Bowdoin, T.; Knapp, D.E.; Anderson, C.; Martin, R.E. Forest Canopy Gap Distributions in the Southern Peruvian Amazon. *PLoS ONE* **2013**, *8*, e60875. [CrossRef]
40. Zhang, Y.; Ma, J.; Liang, S.; Li, X.; Li, M. An Evaluation of Eight Machine Learning Regression Algorithms for Forest Aboveground Biomass Estimation from Multiple Satellite Data Products. *Remote Sens.* **2020**, *12*, 4015. [CrossRef]
41. Gao, Y.; Lu, D.; Li, G.; Wang, G.; Chen, Q.; Liu, L.; Li, D. Comparative Analysis of Modeling Algorithms for Forest Aboveground Biomass Estimation in a Subtropical Region. *Remote Sens.* **2018**, *10*, 627. [CrossRef]
42. Wan-Mohd-Jaafar, W.S.; Woodhouse, I.H.; Silva, C.A.; Omar, H.; Hudak, A.T. Modelling Individual Tree Aboveground Biomass using Discrete Return LiDAR in Lowland Dipterocarp Forest of Malaysia. *J. Trop. For. Sci.* **2017**, *29*, 465–484.
43. Al-Ahmadi, F.; Hames, A. Comparison of Four Classification Methods to Extract Land Use and Land Cover from Raw Satellite Images for Some Remote Arid Areas, Kingdom of Saudi Arabia. *J. King Abdulaziz Univ. Sci.* **2009**, *20*, 167–191. [CrossRef]
44. Nitze, I.; Schulthess, U.; Asche, H. Comparison of Machine Learning Algorithms Random Forest, Artificial Neuronal Network and Support Vector Machine to the Maximum Likelihood for Supervised Crop Type Classification. In Proceedings of the 4th Conference on Geographic Object-Based Image Analysis—GEOBIA, Rio de Janeiro, Brazil, 7–9 May 2012; pp. 35–40.
45. Ellis, P.; Griscom, B.; Walker, W.; Gonçalves, F.; Cormier, T. Mapping selective logging impacts in Borneo with GPS and airborne lidar. *For. Ecol. Manag.* **2016**, *365*, 184–196. [CrossRef]
46. Zhang, J.; Huang, S.; Hogg, E.H.; Lieffers, V.; Qin, Y.; He, F. Estimating spatial variation in Alberta forest biomass from a combination of forest inventory and remote sensing data. *Biogeosciences* **2014**, *11*, 2793–2808. [CrossRef]

47. Adrah, E.; Jaafar, W.S.W.M.; Omar, H.; Bajaj, S.; Leite, R.V.; Mazlan, S.M.; Silva, C.A.; Ooi, M.C.G.; Said, M.N.M.; Maulud, K.N.A.; et al. Analyzing Canopy Height Patterns and Environmental Landscape Drivers in Tropical Forests Using NASA's GEDI Spaceborne LiDAR. *Remote Sens.* **2022**, *14*, 3172. [CrossRef]
48. Jackson, C.; Adam, E. Remote sensing of selective logging in tropical forests: Current state and future directions. *iForest-Biogeosci. For.* **2020**, *13*, 286–300. [CrossRef]
49. Myeong, S.; Nowak, D.J.; Duggin, M.J. A temporal analysis of urban forest carbon storage using remote sensing. *Remote Sens. Environ.* **2006**, *101*, 277–282. [CrossRef]